1. Hocine BENNADJI[1],2. Youcef BEKAKRA[1],3. Saad KHADAR[2], 4.Hamza GASMI[3]

LEVRES Laboratory, Department of Electrical Engineering, Faculty of Technology, University of El Oued, 39000 El Oued, Algeria(1), Laboratory of Applied Automation and Industrial Diagnosis, Ziane Achour University, Djelfa 17000, Algeria (2), Laboratoire de Contrôle Avancé (LABCAV), Department of Electronics and Telecommunications, Université 8 Mai 1945 Guelma, Guelma, Algeria (3)

doi:10.15199/48.2024.06.24

Enhanced sensorless nonlinear control strategy of doubly fed induction motor based on sliding mode observer

Abstract. *This paper presents a sensorless nonlinear control strategy for a doubly fed induction motor (DFIM) based on a combination of backstepping control (BS) and sliding mode observer (SMO) approaches. The main objective is to enhance the performance of field-oriented control (FOC) for DFIM by improving speed control performance, reducing electromagnetic torque ripple and improving stator current distortion, and achieving effective decoupling between torque and stator flux. The stability analysis of the proposed control strategy is conducted using Lyapunov theory. Furthermore, a sliding mode observer is designed to estimate the load torque and motor speed without needing additional sensors. The effectiveness of the proposed control strategy is validated by several simulation tests using Matlab/Simulink software. The results of the first test demonstrate remarkable improvements in response and steady state error of the speed control. Furthermore, the robustness of the designed control strategy is assessed, exhibiting superior performance in speed and torque control, as well as robustness against load disturbances and parameter variations. These findings highlight the potential of the proposed sensorless BS control strategy, with the sliding mode observer, as a promising solution for sensorless control of DFIM in diverse industrial applications.*

Streszczenie. *W artykule przedstawiono bezczujnikową strategię nieliniowego sterowania silnikiem indukcyjnym z podwójnym zasilaniem (DFIM), opartą na połączeniu podejścia ze sterowaniem krokowym (BS) i obserwatorem trybu ślizgowego (SMO). Głównym celem jest zwiększenie wydajności sterowania zorientowanego na pole (FOC) dla DFIM poprzez poprawę wydajności sterowania prędkością, zmniejszenie tętnienia elektromagnetycznego momentu obrotowego i poprawę zniekształceń prądu stojana oraz osiągnięcie skutecznego oddzielenia momentu obrotowego od strumienia stojana. Analizę stabilności zaproponowanej strategii sterowania przeprowadzono z wykorzystaniem teorii Lapunowa. Co więcej, obserwator trybu ślizgowego ma za zadanie szacować moment obciążenia i prędkość silnika bez konieczności stosowania dodatkowych czujników. Skuteczność zaproponowanej strategii sterowania została potwierdzona szeregiem testów symulacyjnych z wykorzystaniem oprogramowania Matlab/Simulink. Wyniki pierwszego testu wykazują niezwykłą poprawę reakcji i błędu stanu ustalonego kontroli prędkości. Ponadto oceniana jest solidność zaprojektowanej strategii sterowania, wykazująca doskonałą wydajność w zakresie sterowania prędkością i momentem obrotowym, a także odporność na zakłócenia obciążenia i zmiany parametrów. Odkrycia te podkreślają potencjał proponowanej bezczujnikowej strategii sterowania BS z obserwatorem w trybie ślizgowym jako obiecującego rozwiązania do bezczujnikowego sterowania DFIM w różnorodnych zastosowaniach przemysłowych.* (***Ulepszona, bezczujnikowa, nieliniowa strategia sterowania silnikiem indukcyjnym z podwójnym zasilaniem, oparta na obserwatorze trybu ślizgowego***)

Keywords: Doubly fed induction motor Backstepping control Sensorless scheme Sliding mode observer Lyapunov theory.
Słowa kluczowe: Silnik indukcyjny podwójnie zasilany Sterowanie cofaniem Schemat bezczujnikowy

Introduction

Nowadays, induction machine drives possess numerous advantageous characteristics over other machinery drives with characteristics like high robustness, low rotor harmonic currents, high power density, low electromagnetic torque pulsations, low per phase current, low MMF harmonics, high reliability, and improved degree of freedom. Among the various types of induction motors, Doubly-Fed Induction Motor (DFIM) has garnered significant attention. The DFIM was first investigated in 1899 as a variable speed motor operating at double synchronous speed and fed on both sides by the network [1], [2], [3]. Over time, several simulation and experimentation studies have been conducted to explore its variable speed control capabilities while DFIMs have been extensively used in generator mode for energy conversion systems, this paper recommends utilizing them in motor mode for high-power applications such as rail traction, marine propulsion, and metallurgy [3], [4], [5].

Despite the numerous advantages of DFIMs, their control poses challenges due to the non-linearity inherent in their mathematical model. Furthermore, their parameters vary over time due to thermal effects and changes in magnetic saturation levels [6], [7].

On the other side, researchers worldwide have devised control techniques of varying complexity, performance, and cost for DFIMs. Traditional vector control techniques, which modify instantaneous voltage and current values, offer excellent dynamic performance and the ability to deliver variable torque similar to independently stimulated DC drives [8]. However, vector control techniques are highly sensitive to parameter changes and external disturbances. Recently, nonlinear techniques have emerged as an intriguing option for replacing the traditional control approach in a variety of systems in order to improve accuracy and precision. Several design approaches based on this theory have been published, including sliding mode control [9]–[11], BS control, and rooted tree optimization algorithms to improve DTC response of DFIM [12]. One of the best nonlinear controls for decoupled control systems that can produce good performance is the BS method [13]–[15]. However, conventional BS control techniques require precise information on both the rotor speed and position, typically obtained using mechanical sensors mounted on the motor shaft. Introducing a sensorless system that estimates speed instead of relying on physical sensors would significantly reduce the cost and complexity of the drive system, considering that sensor costs and maintenance are critical factors for small and medium power drives [1], [16].

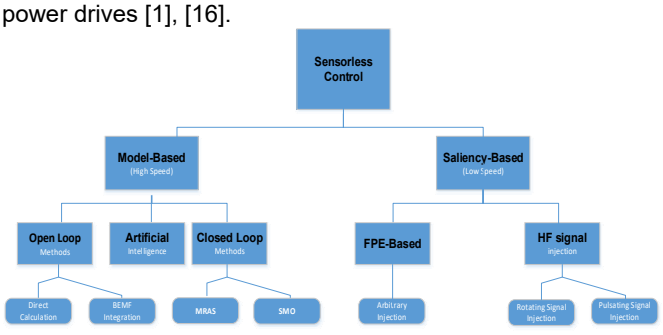

Fig 1. General scheme of sensorless control methods

To eliminate of the position sensor, a lot of attention has been paid during the last few decades to speed estimation techniques to fulfill the requirements of

sensorless control by minimizing the number of mechanical sensors [16]–[18]. These techniques include model reference adaptive systems [1], [8], [19], Luenberger observers [2], Kalman filters [18], [20], sliding mode observers [2], [20]–[22] [23], [24], and neural networks [25]. Among them, sliding mode observers (SMOs) have gained prominence as one of the most effective techniques for sensorless systems is to their reduced complexity and low computational burden, making them well-suited for sensorless motor drives [20], [21], [23], [24].

In light of these considerations, this paper introduces a nonlinear control strategy based on the BS approach for the DFIM. The stability of the control strategy is enhanced using Lyapunov theory. Additionally, a sliding mode observer is employed to estimate of the rotor speed, rotor flux, and load torque. This observer utilizes a simple algorithm compared to previous observers, aiming to minimize the impact of motor parameter variations and ensure accurate speed estimation, particularly in low-speed ranges. The effectiveness and correctness of the proposed control strategy with the examined observers are validated with MATLAB simulations, which demonstrate successful stabilization of speed around desired reference values. Furthermore, the control strategy achieves decoupling between rotor flux and electromagnetic torque, ensuring robust stability under different operating conditions, especially at low-speed ranges.

This paper is organized as follows: Section 2 presents the model of DFIM. Section 3 presents the designed field-oriented control strategy of DFIM. In Section 4, details of the suggested BS approach based on vector control are presented. Section 5 describes the proposed SMO system used for estimating of the motor speed and load torque. To evaluate the effectiveness of this technique, simulation data is presented and analyzed in Section 6. Section 7 provides the conclusion of the paper.

Model Of Doubly-Fed Induction Motor

In order to simplify the differential equations (non-linear) by having constant inductance term, the complexity of the DFIM model is reduced by using the FOC law, where it is assumed that the quadratic stator flux is zero $\varphi_{sq} = 0$, while the direct flux is $\varphi_{sd} = \varphi_s$ [9]. Thus, the DFIM model is described in (*d*-*q*) frames, as follows [11]:

(i.e. the same symbols as in the equations).

Equations

For equations it is recommended to use standard equation editor existing in Word editor (usually it is Math Type editor). The equation editor is defined as follows: font Times New Roman italic, matrix bold, for letters font 10, for index 8, for symbol 12. For example, typical equation should be as:

$$(1)\quad \begin{cases} \dfrac{di_{rd}}{dt} = -\dfrac{A_1 i_{rd}}{\sigma} - A_2 V_{sd} + \dfrac{A_2 \varphi_{sd}}{T_S} + (\omega_s - \omega) i_{rq} + \dfrac{V_{rd}}{\sigma L_r} \\ \dfrac{di_{rq}}{dt} = -\dfrac{A_1 i_{rq}}{\sigma} - A_2 V_{sq} + A_2 \omega \varphi_{sd} - (\omega_s - \omega) i_{rd} + \dfrac{V_{rq}}{\sigma L_r} \end{cases}$$

$$(2)\quad \begin{cases} \dfrac{d\varphi_{sd}}{dt} = V_{sd} + \dfrac{M}{T_S} i_{rd} - \dfrac{1}{T_S} \varphi_{sd} \\ \dfrac{d\Omega}{dt} = \dfrac{PM}{JL_s} (i_{rq} \varphi_{sd}) - \dfrac{C_r}{J} - \dfrac{f}{J} \Omega \end{cases}$$

Electromagnetic torque expression becomes as follows:

$$(3)\quad C_{em} = \frac{P\,\mathrm{M}}{L_s} \varphi_{sd} i_{rq}$$

The values A1 and A2 are defined as follows:

$$(4)\quad \begin{cases} A_1 = \dfrac{1}{T_r} + \dfrac{M^2}{L_s T_s L_r} \\ A_2 = \dfrac{M}{\sigma L_r L_s} \end{cases}$$

where: i_{rd} and i_{rq} are components of rotor current, φ_{sd} and φ_{sq} are components of stator flux, V_{sd} and V_{sq} are stator voltage components, and V_{rd} and V_{rq} are rotor current components. R_s and R_r represent stator and rotor resistances, L_s and L_r represent stator and rotor inductances, M represents mutual inductance, σ is the leakage factor, and P represents the number of pole pairs. C_{em} represents the electromagnetic torque, C_r represents the load torque, J represents the DFIM moment of inertia, Ω is mechanical speed, ω_s represents the stator frequency speed, ω is the rotor frequency speed, and f represents the friction coefficient. T_s and T_r are the statoric and rotoric time constant.

Designed Of Field-Oriented Control Strategy

In the field of motor control, a Proportional-Integral (PI) controller has been widely used to achieve precise speed control and torque regulation. The PI controller combines proportional and integral control actions to drive the motor towards the desired operating conditions. In the case of the DFIM, the PI controller has commonly been employed in the context of the conventional control strategies, such as the field-oriented control (FOC) [15]. FOC aims to decouple the flux and torque control in DFIMs, enabling precise control of motor performance [26]. However, despite its widespread use, the PI controller has some limitations when applied to DFIM control systems. One significant drawback is its susceptibility to external disturbances and sensitivity to variations in system parameters. Changes in the DFIM's rotor resistance and other motor parameters can adversely affect the performance of the PI controller. Moreover, the PI controller may exhibit inadequate response characteristics, including slow response times, steady-state errors, and difficulties in effectively rejecting disturbances. To overcome these limitations, alternative control strategies have been explored to enhance the performance of DFIM control systems. One promising approach is the utilization of advanced control algorithms such as the Sliding Mode Control (SMC). SMC offers robustness and improved control performance for non-linear systems, making it a suitable candidate for enhancing the control of DFIMs.

In the following sections, we will present the mathematical model of the DFIM, discuss the principles of the conventional control strategies, including the PI controller, and introduce the proposed control structure utilizing the SMC to address the limitations of the traditional PI controller in DFIM control systems.

The mathematical model of the PI controller can be expressed as follows:

$$(5)\quad u(t) = K_p e(t) + K_i \int e(t)\, dt$$

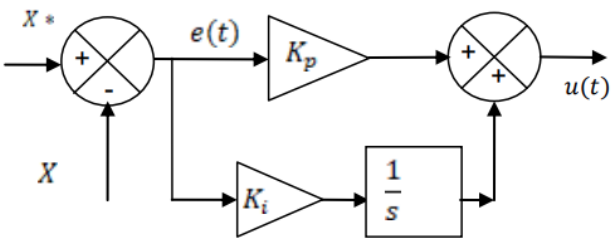

Fig 2. Block diagram of the PI controller

where: $u(t)$ is the control output. $e(t)$ is the error signal between the desired and actual values. K_p is the proportional gain of the controller. K_i is the integral gain of the controller.

Designed of Backstepping Strategy

BS is a recursive control strategy that utilizes virtual controllers designed for each first-order subsystem, serving as a reference for the subsequent controller design stage. The Lyapunov function is employed to ensure tracking accuracy and stability. The BS controller design for DFIMs is conducted in two stages [1], [14], [19], [27], [28].

In the first stage, a reference trajectory is determined for the system, encompassing speed and rotor flux amplitude reference trajectories. The controller design is established to facilitate proper tracking error and trajectory following. This stage sets the foundation for subsequent control design.

In the second stage, the focus shifts towards achieving stabilization and robustness of the control system. Additional controllers are designed to address the remaining dynamics and uncertainties of the DFIM. The aim is to stabilize the system and enhance its robustness against parameter variations, disturbances, and uncertainties.

The specific details of the second stage may vary depending on the particular research or implementation. Various approaches, such as adaptive control, sliding mode control, or other suitable control strategies, can be employed to achieve stabilization and robustness, tailored to the requirements of the DFIM application. By combining trajectory tracking in the first stage and stabilization in the second stage, the two-stage BS controller design offers a comprehensive control strategy. This strategy ensures accurate control, effective disturbance rejection, and robust performance for DFIM systems, making it a valuable approach in various industrial applications. The instantaneous expressions of BS control can be written as follows:

Step 01:

The speed and flux controllers should track the trajectory for input reference. Thus, the errors of speed and flux with their derivative are presented as:

$$\begin{cases} e_1 = \Omega_{ref} - \Omega \\ \dot{e}_1 = \dot{\Omega}_{ref} - \dot{\Omega} \end{cases} \tag{6}$$

$$\begin{cases} e_3 = \varphi_{rdref} - \varphi_{rd} \\ \dot{e}_3 = \dot{\varphi}_{rdref} - \dot{\varphi}_{rd} \end{cases} \tag{7}$$

Based on (1) and (2), the derivative of errors can be established as:

$$\begin{cases} \dot{e}_1 = \dot{\Omega}_{ref} + \dfrac{PM}{JL_S}\left(i_{rq}\varphi_{sd}\right) + \left(\dfrac{C_r}{J} + \dfrac{f}{J}\right)\Omega \\ \dot{e}_3 = \dot{\varphi}_{rdref} - V_{sd} - \dfrac{M}{T_S} i_{rd} + \dfrac{1}{T_S}\varphi_{sd} \end{cases} \tag{8}$$

Lyapunov function is defined as follows:

$$\begin{cases} V = \dfrac{1}{2}e_1^2 + \dfrac{1}{2}e_3^2 \\ \dot{V} = e_1\dot{e}_1 + e_3\dot{e}_3 \end{cases} \tag{9}$$

Thus, the system (9) can be rewritten as:

$$\begin{cases} \dot{V} < 0 \\ \dot{V} = e_1\dot{e}_1 + e_3\dot{e}_3 \end{cases} \tag{10}$$

Substituting (8) in (9), we obtain:

$$\dot{V} = e_1\left[\dot{\Omega}_{ref} + \frac{PM}{JL_S}\left(i_{rq}\varphi_{sd}\right) + \frac{C_r}{J} + \frac{f}{J}\Omega\right] + e_3\left[\dot{\varphi}_{rdref} - V_{sd} - \frac{M}{T_S} i_{rd} + \frac{1}{T_S}\varphi_{sd}\right] \tag{11}$$

The derivative of Lyapunov function gives:

$$\begin{cases} \dot{\Omega}_{ref} + \dfrac{PM}{JL_S}\left(i_{rq}\varphi_{sd}\right) + \dfrac{C_r}{J} + \dfrac{f}{J}\Omega = -K_1 e_1 \\ \dot{\varphi}_{rdref} - V_{sq} - \dfrac{M}{T_s} i_{rd} + \dfrac{1}{T_S}\varphi_{sd} = -K_3 e_3 \end{cases} \tag{12}$$

Then the references currents can be described as:

$$\begin{cases} i_{rqref} = \dfrac{JL_S}{PM\varphi_{sd}}\left[-K_1 e_1 - \dot{\Omega}_{ref} - \dfrac{C_r}{J} - \dfrac{f}{j}\Omega\right] \\ i_{rdref} = \dfrac{T_S}{M}\left[+K_3 e_3 + \dot{\varphi}_{rdref} - V_{sq} + \dfrac{1}{T_S}\varphi_{sd}\right] \end{cases} \tag{13}$$

Step 02:

The goal of this step is to obtain the reference voltages based on the previous phase, where the current errors are obtained as:

$$\begin{cases} e_2 = i_{sqref} - i_{sq} \\ e_4 = i_{sdref} - i_{sd} \end{cases} \tag{14}$$

$$\begin{cases} \dot{e}_2 = \dot{i}_{sqref} - \dot{i}_{sq} \\ \dot{e}_4 = \dot{i}_{sdref} - \dot{i}_{sd} \end{cases} \tag{15}$$

Based on (1) and (2), the derivative of errors can be established as:

$$\begin{cases} \dot{e}_2 = \dot{i}_{sqref} - \left[-\dfrac{1}{\sigma}\left[A_1\right] i_{rq} - A_2 V_{sq} + A_2\omega\varphi_{sd} - \left(\omega_s - \omega\right) i_{rd} + \dfrac{1}{\sigma L_r} V_{rq}\right] \\ \dot{e}_4 = \dot{i}_{sdref} - \left[-\dfrac{1}{\sigma}\left[A_1\right] i_{rd} - A_2 V_{sd} + \dfrac{A_2}{T_S}\varphi_{sd} + \left(\omega_s - \omega\right) i_{rq} + \dfrac{1}{\sigma L_r} V_{rd}\right] \end{cases} \tag{16}$$

Lyapunov function extended is expressed as follow:

$$\begin{cases} V_e = \dfrac{1}{2}e_1^2 + \dfrac{1}{2}e_2^2 + \dfrac{1}{2}e_3^2 + \dfrac{1}{2}e_4^2 \\ \dot{V}_e = e_1\dot{e}_1 + e_2\dot{e}_2 + e_3\dot{e}_3 + e_4\dot{e}_4 \quad \dot{V} = e_2\dot{e}_2 + e_4\dot{e}_4 \end{cases} \tag{17}$$

Thus, the system (17) can be rewritten as:

(18)
$$\begin{cases} \dot{V}_e < 0 \\ \dot{V}_e = -K_2 e_2^2 - K_4 e_4^2 \end{cases}$$

Substituting (16) in (17), we obtain:

(19)
$$\begin{cases} \dot{i}_{sqref} + \frac{1}{\sigma}[A_1] i_{rq} + A_2 V_{sq} - A_2 \omega \varphi_{sd} + (\omega_s - \omega) i_{rd} - \frac{1}{\sigma L_r} V_{rq}] = -K_2 e_2 \\ \dot{i}_{sdref} + \frac{1}{\sigma}[A_1] i_{rd} + A_2 V_{sd} - \frac{A_2}{T_S} \varphi_{sd} - (\omega_s - \omega) i_{rq} - \frac{1}{\sigma L_r} V_{rd}] = -K_4 e_4 \end{cases}^T$$

hen the references voltages can be described as:

(20)
$$\begin{cases} V_{rq} = \sigma L_r \left[\dot{i}_{sqref} - \frac{1}{\sigma}[A_1] i_{rq} + A_2 V_{sq} - A_2 \omega \varphi_{sd} + (\omega_s - \omega) i_{rd} + K_2 e_2 \right] \\ V_{rd} = \sigma L_r \left[\dot{i}_{sdref} + \frac{1}{\sigma}[A_1] i_{rd} + A_2 V_{sd} - \frac{A_2}{T_S} \varphi_{sd} - (\omega_s - \omega) i_{rq} + K_4 e_4 \right] \end{cases}$$ **Sliding**

Mode Observer

A sliding mode observer (SMO) is a valuable tool in control theory for estimating the state of a system, particularly in cases where direct measurement is challenging or costly. The fundamental concept behind a sliding mode observer is to employ a sliding mode control approach to construct an observer that closely tracks the system's state. By minimizing the discrepancy between the observed and actual state variables, the observer generates state estimates [20] [21].

The distinguishing feature of a SMO is its operation in sliding mode, where the dynamics of the observer error are designed to converge to zero within a finite time. This property enables the observer to provide accurate state estimates even in the presence of system uncertainties or noise. As a result, sliding mode observers are frequently utilized in sensorless control applications for electrical machines like motors, as they allow estimation of crucial parameters such as rotor position and speed without requiring direct measurement. By leveraging the principles of sliding mode control and exploiting the robustness properties of sliding mode observers, accurate and reliable state estimation can be achieved in various real-world scenarios. The use of sliding mode observers in sensorless control applications contributes to cost reduction, enhanced system performance, and increased reliability in electrical machine systems.

Speed observer

Sliding mode observer expressed in (34) can be used to calculate speed [11], [26] as:

(21)
$$\hat{\dot{\omega}}_r = -\frac{f}{J}\omega_r + \frac{1}{J}C_{em} - \frac{1}{J}\hat{C}_r + \lambda_1 e_\omega + K_1 sign(e_\omega)$$

Load torque observer

A load torque observer (LTO) is a valuable component in motor control systems as it enables the estimation of the load torque on the motor shaft without the use of a torque sensor [21], [24]. This is particularly useful in situations where the load torque is unknown or variable, as it helps to improve control performance by reducing system uncertainty [19], [26]–[28], [28], [29].

Typically, a torque sensor is employed to directly measure the load torque, providing accurate information about the system. However, in cases where a torque sensor is not available or impractical to use, the LTO serves as an alternative solution. By employing a sliding mode observer, the applied load torque on the induction motor can be estimated without the need for a torque sensor. This estimation helps to reduce system uncertainty and enhance control performance [19], [26]–[28], [29].

In this paper, the proposed approach utilizes a sliding mode observer to estimate the applied load torque on the induction motor. By considering the unknown or variable load torque as a source of system uncertainty, the observer is designed to minimize the discrepancy between the estimated and actual values. This estimation of the load torque contributes to improved control performance, enabling the motor control system to respond effectively to changes in the load and achieve desired operation. The mechanical model of the induction motor is utilized in the development of the load torque observer. By considering the dynamic equations of the DFIM and accounting for the unknown parameters, the observer is able to estimate the load torque accurately. Overall, the incorporation of a sliding mode observer for load torque estimation in the motor control system presents a valuable approach to reduce system uncertainty and enhance control performance [21], [29]–[31], [31], [32]. By eliminating the need for a torque sensor, the proposed method offers a cost-effective and reliable solution for estimating the applied load torque, leading to more effective motor control in various applications. The mechanical model of the DFIM is as follows:

$$\begin{cases} \dot{\omega}_r = -\frac{f}{J}\omega_r + \frac{1}{J}C_{em} - \frac{1}{J}C_r \\ \dot{C}_r = 0 \end{cases}$$

(22) The speed estimation error is represented by the sliding surface: e_W the estimation errors are calculated as follows:

$$\begin{cases} e_\omega = (\omega_r - \hat{\omega}_r) \\ e_{Cr} = (C_r - \hat{C}_r) \end{cases}$$

(23)

where: e_W: error in load torque estimation, e_{Cr}: error in load torque estimation.

$$\begin{cases} \dot{e}_\omega = \frac{1}{J}e_{Cr} - \lambda_1 e_\omega - K_1 sign(e_\omega) \\ \dot{e}_{Cr} = \lambda_2 e_\omega + K_2 sign(e_\omega) \end{cases}$$

(24)

where: K_1, K_2, λ_1 and λ_2 are positive constants. If the observer gains are big enough to satiate the stability condition, the estimation error converges to zero.

1. SIMULATION RESULTS AND INTERPRETATIONS

In order the DFIM is subjected to robustness tests for variable operating conditions to verify the performance and stability of the control system via the sensorless strategy BS control.

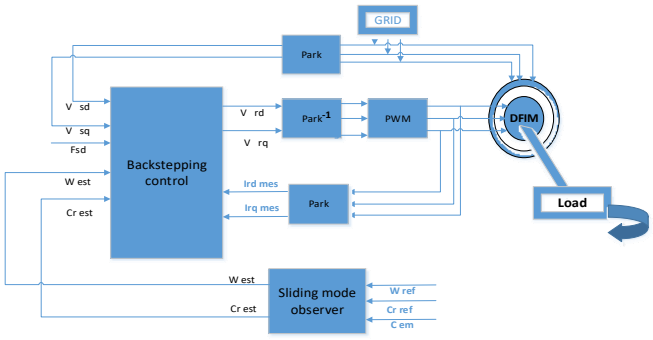

Fig 3. Schematic of a sensorless BS control strategy for a DFIM with SMO

The operation of the DFIM was tested using a trajectory that encompassed various operating conditions by applying and removing a load of [0 5 0 5 0 0] N.m at [0 0.75 1.75 2.75 4.25 4.5] [sec]. The numerical simulation of the observer control machine set was conducted to assess the performance of the system. The simulation tests were performed on a DFIM with parameters outlined in Table 1.

Table 1. Parameters of a 0.8kW DFIM

Parameter	**Value**
Stator peak phase voltage	380V
Rotor resistance	11.98 Ω
Stator resistance	0.904 Ω
Rotor inductance	0.0556 H
Stator inductance	0.414 H
Magnetizing inductance	0.126 H
Number of pair of poles	2
Moment of inertia	0.01 kg.m²
Viscous friction coefficient	0.01 N.m.s/rad

In Figure 4, the system responses are presented for a speed setpoint of [0 0 20 20 100 100 -15 -15 0 0] [rad/sec] at corresponding time intervals [0 0.5 0.6 1.4 1.8 2.8 3.3 3.9 4 4.5] [sec]. Figure 4 provides a clear visualization of the rotor speed variations and their corresponding time evolution, demonstrating the system's response to load changes. The rotor speed of the DFIM exhibits excellent tracking performance with both the proposed BS controller and the conventional PI controller. In both cases, the rotor speed closely follows the reference speed, indicating effective speed control. Additionally, the estimated speed obtained from the sliding mode observer and the PI controller aligns closely with the controlled speed. This demonstrates that the speed estimation provided by the SMO is accurate and reliable, comparable to the estimation achieved by the PI controller.

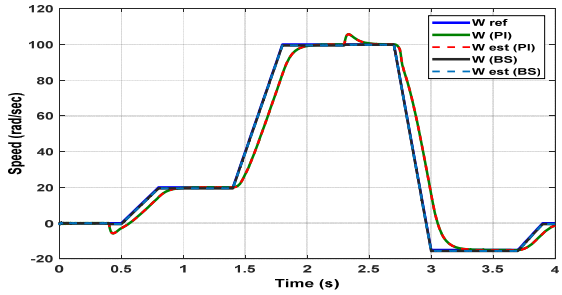

Fig 4. Rotor speed

Figure 5 shows that the proposed BS combined with the SMO outperforms the conventional PI controller in terms of response time, and steady-state error. The BS controller exhibits faster response, resulting in reduced rise time and response time compared to the PI controller. Additionally, the steady-state error of the BS controller is lower, indicating better tracking of the desired speed reference. These improvements demonstrate the effectiveness of the proposed control strategy in achieving faster response and more accurate speed control compared to the conventional PI controller.

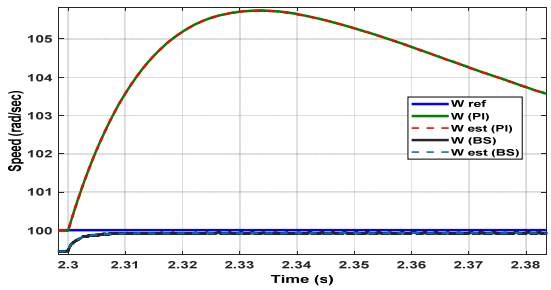

Fig 5. Zoom in rotor speed

As shown in Figures 6 and 7, the BS and PI controller reveals significant improvements in torque control and estimation. The BS controller outperforms the PI controller in terms of response time and oscillation reduction, leading to more precise and stable torque control. The BS controller demonstrates superior performance by minimizing torque ripples and achieving faster response times compared to the PI controller. It effectively tracks the desired torque trajectory, ensuring rapid adjustments to load variations and disturbances. Additionally, the torque estimation obtained by the BS controller exhibits remarkable accuracy and closely follows the actual torque.

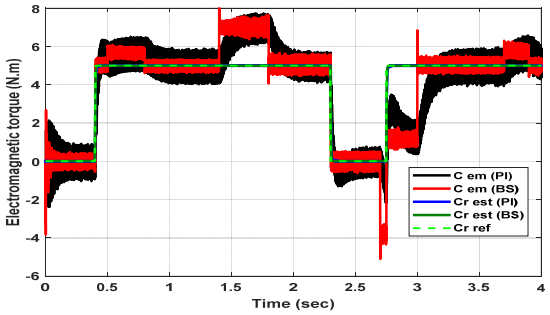

Fig 6. Electromagnetic torque

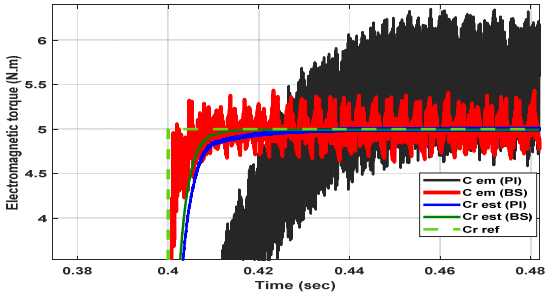

Fig 7. Zoom in electromagnetic torque

Figures 8, 9 and 10 show the stator currents obtained by both BS and PI controllers exhibit sinusoidal shapes, indicating accurate regulation and tracking of the reference values. The BS controller shows improved performance in terms of minimizing oscillations and achieving smoother current profiles compared to the PI controller.

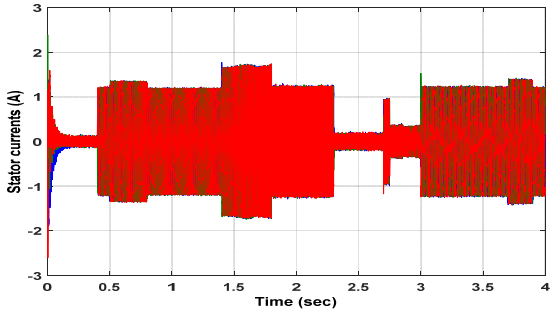

Fig 8. Stator currents obtained by PI controller

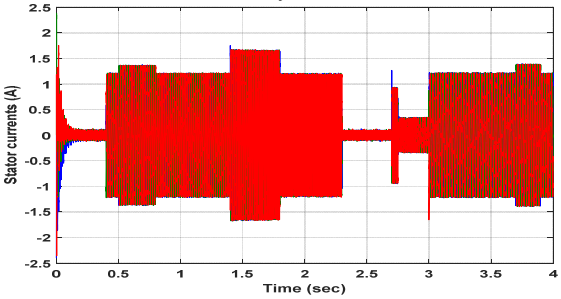

Fig 9. Stator currents obtained by BS controller

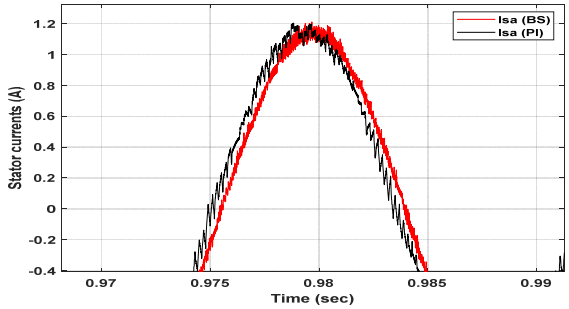

Fig 10. Zoom in stator currents

Figure 11 shows the stator flux, it has a fast response, good reference tracking (1Wb) for both techniques. However, the stator flux obtained by BS technique is more close to the reference compared with the conventional technique.

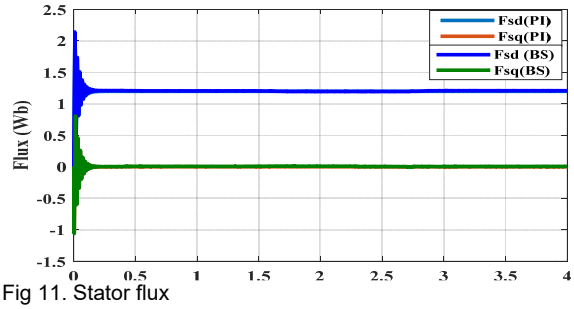

Fig 11. Stator flux

Total harmonic distortion (THD) analysis of the stator current reveals that the proposed BS controller outperforms the conventional PI controller in terms of reducing harmonic components. Figures 12 and 13 illustrate the THD values for the stator current obtained by both controllers. It can be observed that the BS controller achieves a significantly lower THD value compared to the PI controller. Specifically, the THD reduction achieved by the BS controller amounts to 9.52% compared to the conventional PI controller (15.32%). This highlights the superior performance of the proposed BS controller in minimizing harmonic distortions and improving the quality of the stator current.

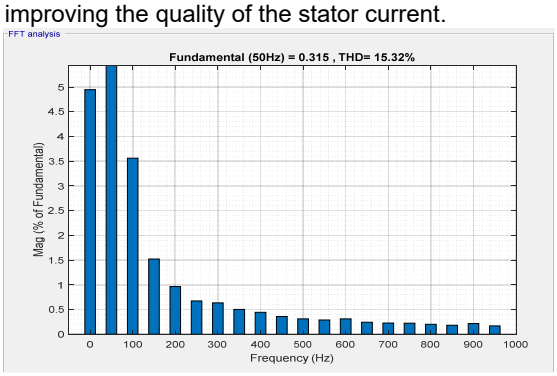

Fig 12. THD value of stator currents obtained by PI controller

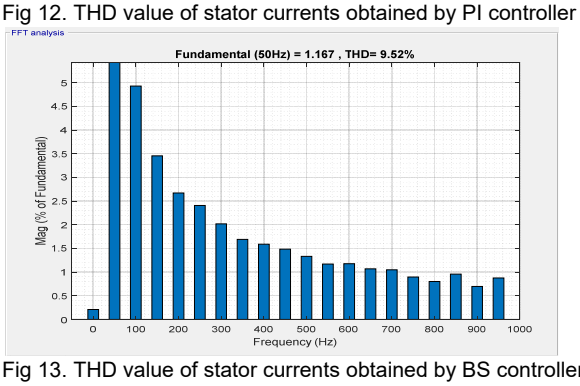

Fig 13. THD value of stator currents obtained by BS controller

Conclusion

In this paper, an improved non-linear sensorless control strategy based on backstepping control (BS) and sliding mode observer techniques was proposed for motor mode operation of a doubly fed induction motor (DFIM). The integrated control system demonstrated robust performance, accurate speed and torque control, and improved stability compared to conventional approach.

The results highlighted the advantages of the proposed control strategy, including reduced response time, steady-state error and torque oscillation compared to the conventional PI controller. The BS combined with sliding mode observer yielded precise speed tracking and enhanced disturbance rejection, particularly during load variations.

Future research can focus on addressing implementation challenges, such as system complexity and real-time computational requirements, as well as exploring the performance of the control strategy under specific operating conditions and its application to different motor types. Overall, the presented non-linear sensorless control strategy based on BS and sliding mode observer techniques offers a promising solution for achieving precise and robust control of DFIM in motor mode. Its superior performance in terms of speed tracking, disturbance rejection, and stability paves the way for improved efficiency and reliability in various industrial applications.

REFERENCES

[1] K. Saad, K. Abdellah, H. Ahmed, and A. Iqbal, “Investigation on SVM-Backstepping sensorless control of five-phase open-end winding induction motor based on model reference adaptive system and parameter estimation,” *Engineering Science and Technology, an International Journal*, vol. 22, no. 4, pp. 1013–1026, 2019.

[2] H. Echeikh, R. Trabelsi, A. Iqbal, and M. F. Mimouni, “Adaptive direct torque control using Luenberger-sliding mode observer for online stator resistance estimation for five-phase induction motor drives,” *Electr Eng*, vol. 100, no. 3, pp. 1639–1649, Sep. 2018.

[3] S. Drid, M. Nait-Said, and M. Tadjine, “Double flux oriented control for the doubly fed induction motor,” *Electric Power Components and Systems*, vol. 33, no. 10, pp. 1081–1095, 2005.

[4] M. Zerzeri and A. Khedher, “Optimal speed–torque control of doubly-fed induction motors: Analytical and graphical analysis,” *Computers & Electrical Engineering*, vol. 93, p. 107258, 2021.

[5] Y. Azzoug, M. Sahraoui, R. Pusca, T. Ameid, R. Romary, and A. J. M. Cardoso, “High-performance vector control without AC phase current sensors for induction motor drives: Simulation and real-time implementation,” *ISA Transactions*, vol. 109, pp. 295–306, Mar. 2021, doi: 10.1016/j.isatra.2020.09.021.

[6] M. Mounira and C. Djamila, “A new approach of robust speed-sensorless control of doubly fed induction motor fed by photovoltaic solar panel,” *IJPEDS*, vol. 14, no. 1, p. 153, Mar. 2023, doi: 10.11591/ijpeds.v14.i1.pp153-166.

[7] S. Drid, M. Nait-Said, and M. Tadjine, “Double flux oriented control for the doubly fed induction motor,” *Electric Power Components and Systems*, vol. 33, no. 10, pp. 1081–1095, 2005.

[8] I. Benlaloui, S. Drid, L. Chrifi-Alaoui, and M. Ouriagli, “Implementation of a New MRAS Speed Sensorless Vector Control of Induction Machine,” *IEEE Trans. Energy Convers.*, vol. 30, no. 2, pp. 588–595, Jun. 2015.

[9] Y. Bekakra and D. B. Attous, “Fuzzy sliding mode controller for doubly fed induction motor speed control,” *Journal of Fundamental and Applied Sciences*, vol. 2, no. 2, pp. 272–287, 2010.

[10] Y. Bekakra and D. B. Attous, “A sliding mode speed and flux control of a doubly fed induction machine,” presented at the 2009 International Conference on Electrical and Electronics Engineering-ELECO 2009, IEEE, 2009, p. I–174.

[11] C. Djamila and Y. Miloud, “High performance of sensorless sliding mode control of doubly fed induction motor associated

with two multilevel inverters fed by VFDPC_SVM rectifier," *Indonesian Journal of Electrical Engineering and Informatics (IJEEI)*, vol. 8, no. 2, pp. 242–255, 2020.
[12] Y. Bekakra, Y. Labbi, D. Ben Attous, and O. P. Malik, "Rooted Tree Optimization Algorithm to Improve DTC Response of DFIM," *J. Electr. Eng. Technol.*, vol. 16, no. 5, pp. 2463–2483, Sep. 2021.
[13] T. Ameid, A. Menacer, H. Talhaoui, A. Ammar, and Y. Azzoug, "Sensorless speed estimation and backstepping control of induction motor drive using model reference adaptive system," presented at the 2017 5th International Conference on Electrical Engineering-Boumerdes (ICEE-B), IEEE, 2017, pp. 1–6.
[14] D. Traoré, J. de Leon, and A. Glumineau, "Sensorless induction motor adaptive observer-backstepping controller: experimental robustness tests on low frequencies benchmark," *IET control theory & applications*, vol. 4, no. 10, pp. 1989–2002, 2010.
[15] M. Taoussi, M. Karim, D. Hammoumi, C. El Bekkali, B. Bossoufi, and N. El Ouanjli, "Comparative study between Backstepping adaptive and Field-oriented control of the DFIG applied to wind turbines," presented at the 2017 International Conference on Advanced Technologies for Signal and Image Processing (ATSIP), IEEE, 2017, pp. 1–6.
[16] N. El Ouanjli *et al.*, "Real-time implementation in dSPACE of DTC-backstepping for a doubly fed induction motor," *The European Physical Journal Plus*, vol. 134, pp. 1–14, 2019.
[17] K. Kroics and H. Hafezi, "An Accurate Mechanical Overload Detection for Induction Motor via Sensorless Load Torque Estimation," in *2021 IEEE 62nd International Scientific Conference on Power and Electrical Engineering of Riga Technical University (RTUCON)*, Riga, Latvia: IEEE, Nov. 2021, pp. 1–5.
[18] A. Chibah, M. Menaa, K. Yazid, A. Boufertella, H. Djadi, and M. Boudour, "A new sensorless control of doubly fed induction motor based on extended complex kalman filter," presented at the 2018 International Conference on Electrical Sciences and Technologies in Maghreb (CISTEM), IEEE, 2018, pp. 1–6.
[19] T. Ameid, A. Menacer, H. Talhaoui, A. Ammar, and Y. Azzoug, "Sensorless speed estimation and backstepping control of induction motor drive using model reference adaptive system," presented at the 2017 5th International Conference on Electrical Engineering-Boumerdes (ICEE-B), IEEE, 2017, pp. 1–6.
[20] H. Majid and H. Abouaïssa, "Comparative Study of a Super-Twisting Sliding Mode Observer and an Extended Kalman Filter for a Freeway Traffic System," *Cybernetics and Information Technologies*, vol. 15, no. 2, pp. 141–158, Jun. 2015.
[21] A. Ammar, A. Bourek, and A. Benakcha, "Sensorless SVM-direct torque control for induction motor drive using sliding mode observers," *Journal of Control, Automation and Electrical Systems*, vol. 28, no. 2, pp. 189–202, 2017.
[22] S. A. Davari, D. A. Khaburi, F. Wang, and R. Kennel, "Robust sensorless predictive control of induction motors with sliding mode voltage model observer," *Turkish Journal of Electrical Engineering and Computer Sciences*, vol. 21, no. 6, pp. 1539–1552, 2013.
[23] N. K. M'Sirdi, A. Rabhi, L. Fridman, J. Davila, and Y. Delanne, "Second order sliding-mode observer for estimation of vehicle dynamic parameters," *IJVD*, vol. 48, no. 3/4, p. 190, 2008.
[24] Zhang, Y., Yin, Z., Liu, J. and Tong, X., 2018. Design and implementation of an adaptive sliding-mode observer for sensorless vector controlled induction machine drives. Journal of Electrical Engineering & Technology, 13(3), pp.1304-1316. [25] P. Georgieva and S. F. de Azevedo, "Neural networks for model predictive control," presented at the The 2011 International Joint Conference on Neural Networks, IEEE, 2011, pp. 111–118.
[26] H. Benderradji, A. Makouf, and L. Chrifi-Alaoui, "Field-oriented control using sliding mode linearization technique for induction motor," in *18th Mediterranean Conference on Control and Automation, MED'10*, Marrakech, Morocco: IEEE, Jun. 2010, pp. 1133–1138.
[27] de Leon, J., Souleiman, I., Glumineau, A. and Schreier, G., 2001. On nonlinear equivalence and backstepping observer. Kybernetika, 37(5), pp.521-546.
[28] J. Soltani, A. F. Payam, and M. A. Abbasian, "A speed sensorless sliding-mode controller for doubly-fed induction machine drives with adaptive backstepping observer," presented at the 2006 IEEE International Conference on Industrial Technology, IEEE, 2006, pp. 2725–2730.
[29] A. Ammar, "Second-order sliding mode-direct torque control and load torque estimation for sensorless model reference adaptive system–based induction machine," *Proceedings of the Institution of Mechanical Engineers, Part I: Journal of Systems and Control Engineering*, vol. 235, no. 1, pp. 15–29, Jan. 2021.
[30] G. Bartolini, A. Damiano, G. Gatto, I. Marongiu, A. Pisano, and E. Usai, "Robust speed and torque estimation in electrical drives by second-order sliding modes," *IEEE Trans. Contr. Syst. Technol.*, vol. 11, no. 1, pp. 84–90, Jan. 2003.
[31] L. Aarniovuori, H. Karkkainen, M. Niemela, P. Lindh, and J. Pyrhonen, "Induction motor torque estimation accuracy using motor terminal variables," in *2017 IEEE International Electric Machines and Drives Conference (IEMDC)*, Miami, FL: IEEE, May 2017, pp. 1–7.
[32] A. Goedtel, I. Nunes Da Silva, P. J. Amaral Serni, and E. Avolio, "Load torque estimation in induction motors using artificial neural networks," in *Proceedings of the 2002 International Joint Conference on Neural Networks. IJCNN'02 (Cat. No.02CH37290)*, Honolulu, HI, USA: IEEE, 2002, pp. 1379–1384.